

# Wind-driven coastal sea level variability in the Northeast Pacific

OSTST Meeting, Boulder, CO, October 2013

Philip R. Thompson<sup>1,2</sup>, Mark A. Merrifield<sup>1,2</sup>, Judith R. Wells<sup>2</sup>, and Chantel M. Chang<sup>2</sup>

<sup>1</sup>Department of Oceanography, SOEST, University of Hawai'i at Mānoa, Honolulu, HI, USA

<sup>2</sup>Joint Institute for Marine and Atmospheric Research, Honolulu, HI, USA

Email: philiprt@hawaii.edu

Citation: Thompson, P. R., M. A. Merrifield, J. R. Wells, and C. M. Chang (2013), Wind-driven coastal sea level variability in the Northeast Pacific, *Submitted to Journal of Climate (in review)*.



## Introduction

The link between the enhanced rates of sea level change in the Western Tropical Pacific and intensified trade winds has received much attention<sup>1</sup>, but the role of wind-forcing in recent near-zero rates along the Northeast Pacific (NEP) coast (Figure 1) is not clear. Sea level variability along the NEP coast is dominated by coastally trapped waves of tropical origin south of San Francisco with large-scale, longshore winds becoming increasingly important to the north<sup>2,3</sup>. Another possible driver of NEP sea level variability is wind-stress-curl (WSC), which is known to be a primary driver of open ocean variability<sup>4,5</sup>. The relationship between WSC and coastal sea level is less clear, however, as there is evidence both for<sup>6</sup> and against<sup>3</sup> the role of WSC as a leading-order driver of coastal sea level variability in the NEP region. The purpose of this work is to assess the relative roles of various wind-forcing mechanisms in the decline of NEP sea level change rates during recent decades.

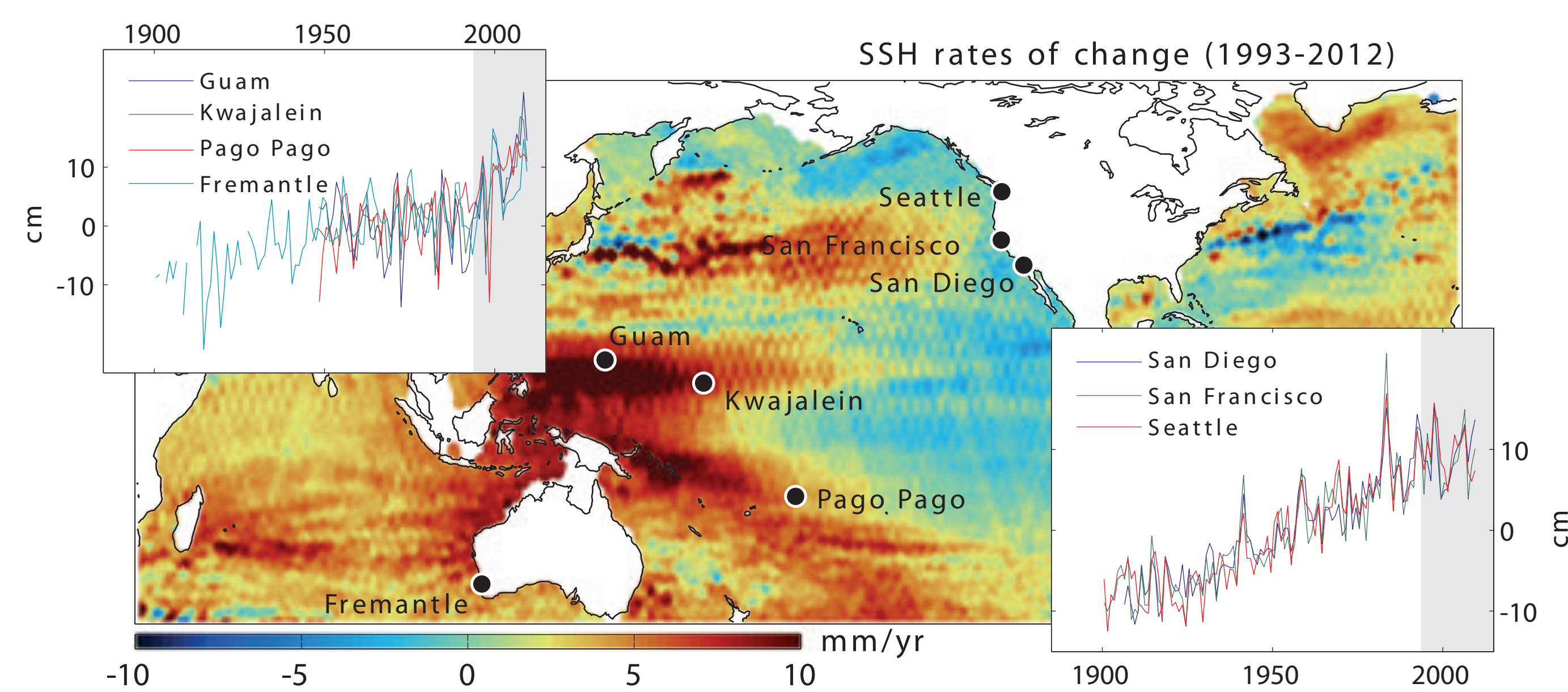


Figure 1: Linear rates of sea surface height (SSH) change measured by satellite altimeters and annually averaged coastal sea level anomalies from selected North Pacific tide gauges.

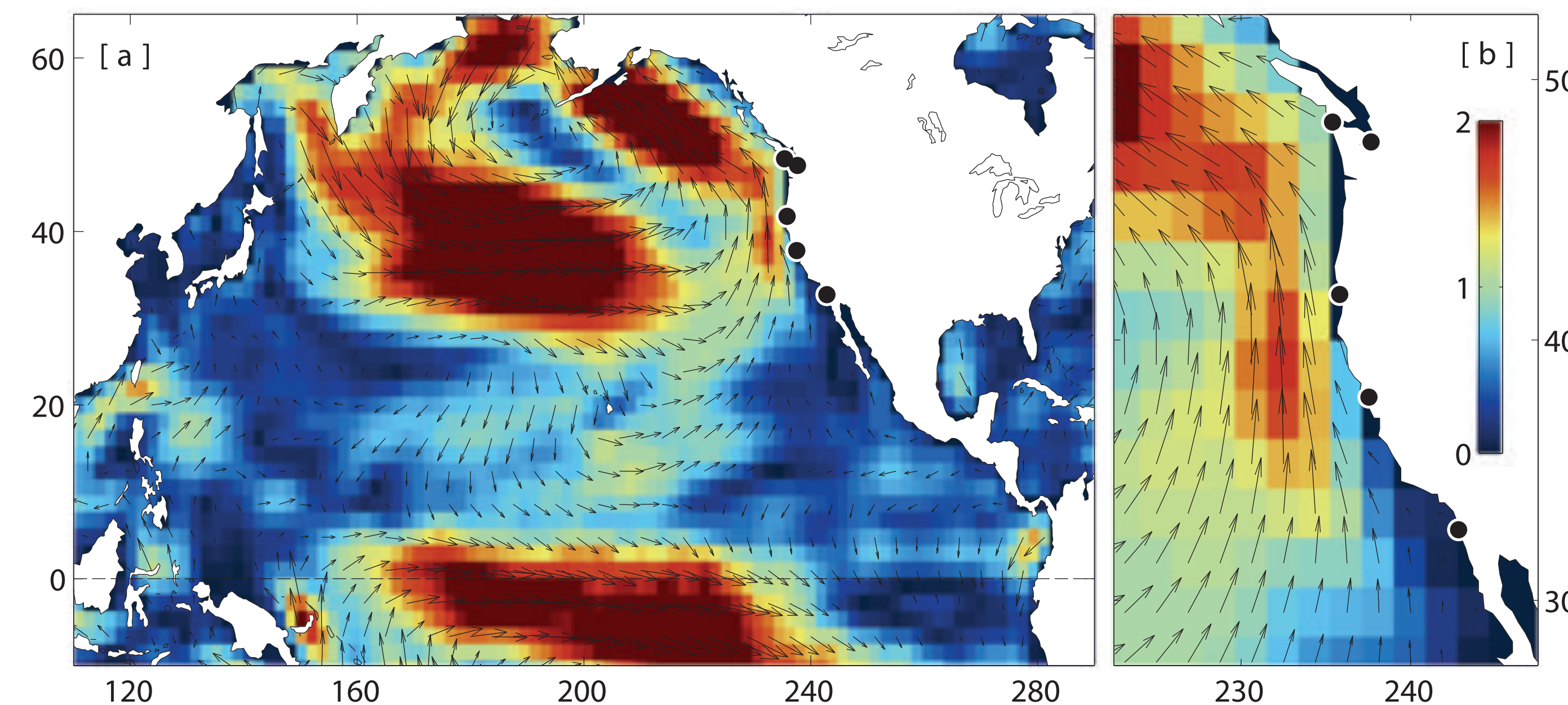


Figure 2: [a] Vector combinations of zonal and meridional regression coefficients for regressions of annual average wind-stress onto  $\tau_{eq}$  (arrows) and the magnitude of the vectors (colors). [b] Same as [a], but with increased detail near the tide gauges of interest. The regression coefficients are unitless, and the color bar in [b] applies to both panels.

## Regressions north of San Diego

The product  $a_{sd}\tau_{eq}$  represents sea level variability at San Diego resulting from equatorially forced anomalies, and in order to circumvent the correlation between  $\tau_{eq}$  and  $\tau_{ls}$  in regressions at gauges further to the north, we assume this equatorially forced variability is constant at all gauges. This assumption is reasonable as the largest amplitude coastally-trapped propagating anomalies are coherent north of the Gulf of California. Little longshore difference in amplitude is found in either altimetry<sup>7,8</sup> or high-resolution models<sup>9,10</sup>. The regression then takes the form

$$[\eta - a_{sd}\tau_{eq}] = \eta + b\tau_{ls} + c\tau_{xy} + \epsilon.$$

The results of these regressions (Figures 4 & 5) suggest that although local longshore winds are an important driver of coastal sea level variability and can account for a majority of the variability in annual averaged sea levels, the recent suppression of sea level rise along the NEP coastline is of primarily tropical origin resulting from adjustment along the wave-guide to anomalous equatorial wind-stress. This mechanism is further supported by the the relationship between long-term trends at San Diego in the east and Fremantle in the west (Figure 6).

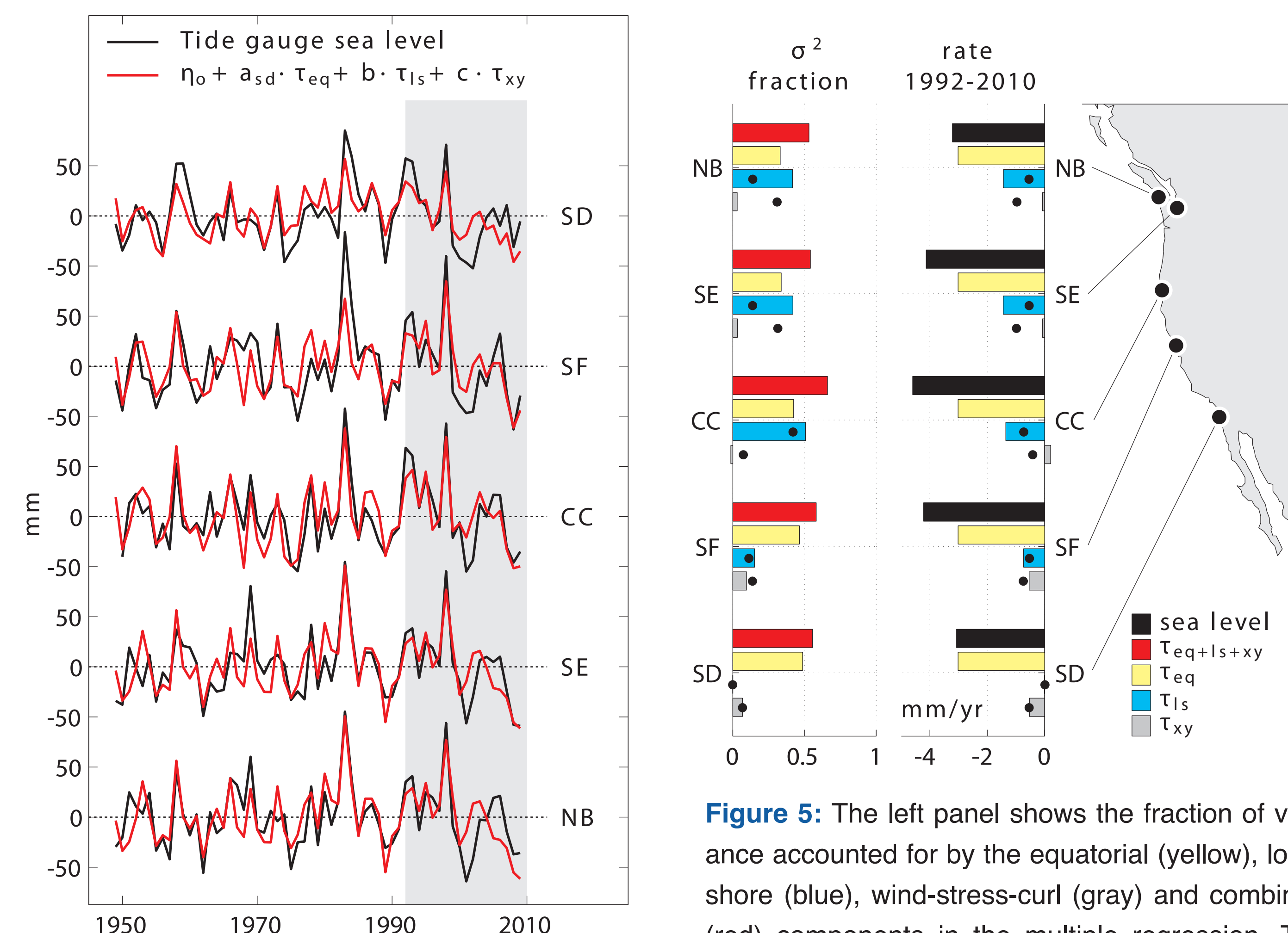


Figure 5: The left panel shows the fraction of variance accounted for by the equatorial (yellow), longshore (blue), wind-stress-curl (gray) and combined (red) components in the multiple regression. The right panel shows linear rates of change during the altimeter period for the measured sea levels (black bar) and estimates of each contribution to the rate from the individual wind-forced components.

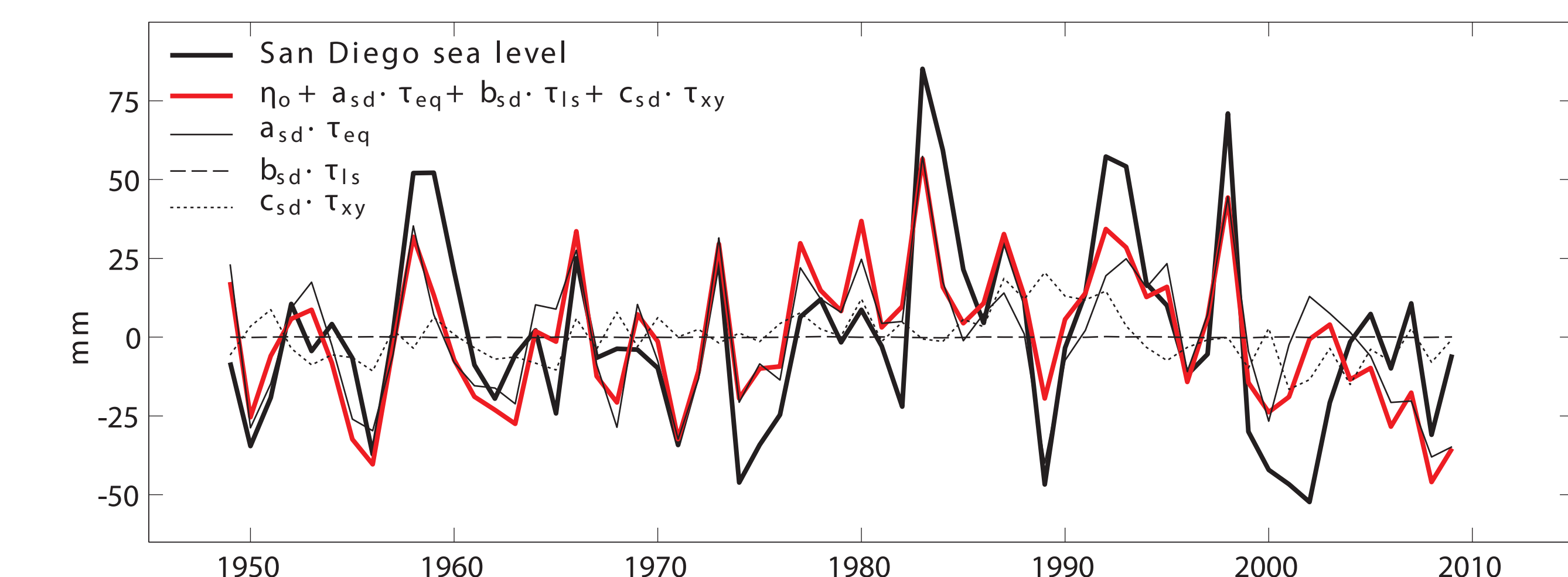


Figure 3: Detrended San Diego sea level (minus reconstructed global mean sea level) and the result of a multiple linear regression onto equatorial wind-stress ( $\tau_{eq}$ ), longshore wind-stress ( $\tau_{ls}$ ), and local wind-stress curl ( $\tau_{xy}$ ).

## Regression at San Diego

The principal difficulty in statistically separating the relative contributions of various wind-forced mechanisms is the correlation between equatorial wind-stress ( $\tau_{eq}$ ), longshore wind-stress ( $\tau_{ls}$ ), and local wind-stress curl ( $\tau_{xy}$ ). This relationship is illustrated in Figure 2, which shows regressions of zonal and meridional wind-stress over the Pacific onto  $\tau_{eq}$ . The signature of the Aleutian Low is apparent, such that weaker than normal equatorial trades (i.e., El Niño conditions) correspond to a deepened Aleutian Low and increased longshore wind-stress along the NEP coastline.

The detailed view of the west coast of the United States (Figure 2b) shows that longshore winds at San Diego do not correlate with  $\tau_{eq}$  due to the orientation of the coastline and the cyclonic structure of the Aleutian Low. The independence of  $\tau_{eq}$  and  $\tau_{ls}$  at San Diego allows for statistical separation in a regression. There is a small correlation between  $\tau_{xy}$  and  $\tau_{eq}$  that is removed by subtracting the correlated variability from  $\tau_{eq}$ . This gives three independent inputs for a multiple linear regression (MLR) at San Diego. The result of the MLR (Figure 3) shows that the recent trend in coastal sea level at San Diego is mostly accounted for by  $\tau_{eq}$ .

## Conclusions

- 1) The recent thickening of the upper layer in the western Pacific is a response to intensified trade winds that must be compensated by a thinning of the upper layer elsewhere. This adjustment occurs along the equatorial and coastal waveguides and is found via statistical methods to be the leading cause of the recent reduction in the rate of NEP coastal sea level change.
- 2) Long-term predictability of NEP coastal sea level variability is therefore more closely tied to tropical winds than extratropical winds.
- 3) Volume redistribution in the North Pacific due to tropical forcing gives the impression that sea level change is decelerating along the NEP coastline<sup>11</sup>. Accounting for regional variability changes the sign of the acceleration to positive with values consistent with the acceleration in GMSL over the same period (Table 1).

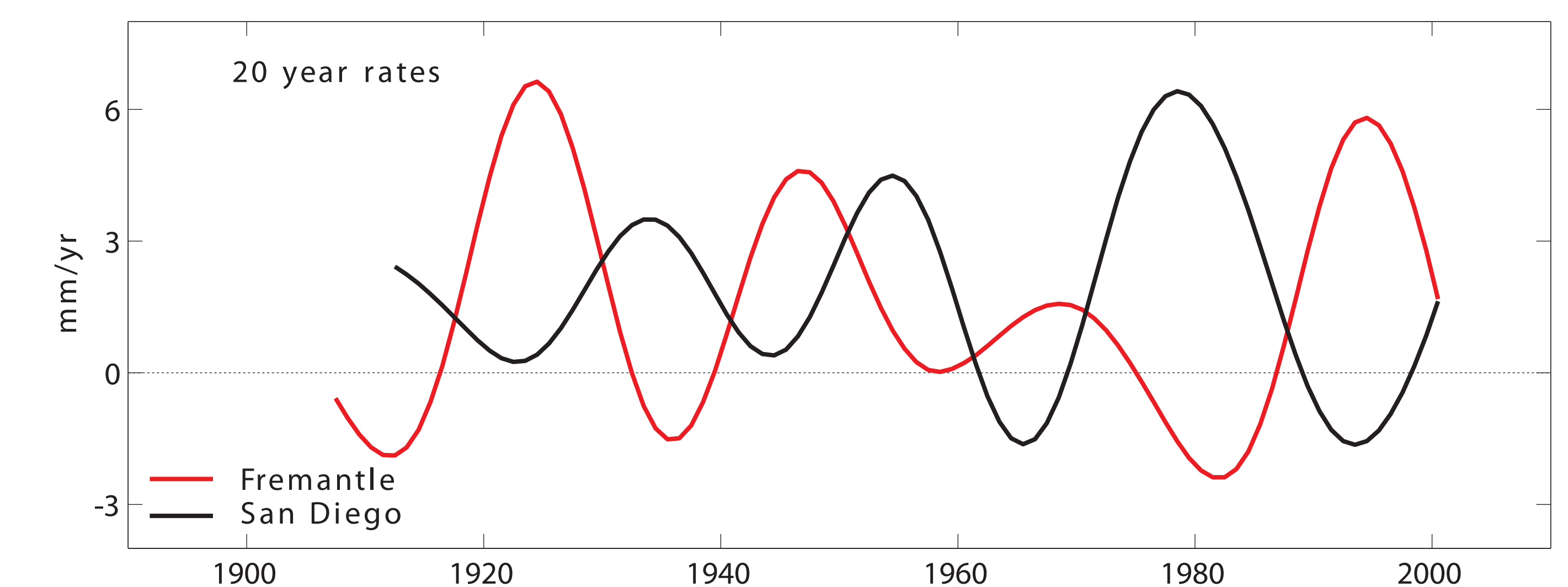


Figure 6: Twenty year sea level change rates from San Diego (black) and Fremantle (red).

	SD	SF	CC	SE	NB	
Houston and Dean (2011)	-0.010	-0.022	-0.014	-0.032	-0.038	mm-yr <sup>-2</sup>
$\eta_{lg}$	-0.023	-0.049	-0.014	-0.026	-0.050	mm-yr <sup>-2</sup>
$\eta_{lg} - \eta_{ws}$	0.043	-0.004	0.018	0.019	0.044	mm-yr <sup>-2</sup>

Table 1: Acceleration coefficients during the period 1948-2010 from a linear least squares fit to a quadratic for annually averaged Northeast Pacific sea level anomalies ( $\eta_{lg}$ ) and anomalies minus estimated regional wind-driven variability ( $\eta_{lg} - \eta_{ws}$ ). Also shown are acceleration coefficients during the 1930-2010 period or entire record, whichever is shorter, from Houston & Dean (2011).

## Data

Annual sea level time series are calculated using monthly mean tide gauge sea levels from the Permanent Service for Mean Sea Level (PSMSL, <http://www.psmsl.org>) after removing the mean annual cycle and correcting for the inverted barometer effect. Wind-stress fields (1948-2010) are obtained from the NCEP/NCAR Reanalysis 1 (NCEP1) project.

## References

- <sup>1</sup>Merrifield, M. A., 2011: A Shift in Western Tropical Pacific Sea Level Trends during the 1990s. *Journal of Climate*, 24 (15), 4126-4138.
- <sup>2</sup>Enfield, D. B. and J. S. Allen, 1980: On the Structure and Dynamics of Monthly Mean Sea Level Anomalies along the Pacific Coast of North and South America. *Journal of Physical Oceanography*, 10 (4), 557-578.
- <sup>3</sup>Chelton, D. B. and R. E. Davis, 1982: Monthly Mean Sea-Level Variability Along the West Coast of North America. *Journal of Physical Oceanography*, 12 (8), 757-784.
- <sup>4</sup>Lagerloef, G. S. E., 1995: Interdecadal variations in the Alaska Gyre. *Journal of Physical Oceanography*, 25, 2242-2258.
- <sup>5</sup>Fu, L. L. and B. Qiu, 2002: Low-frequency variability of the North Pacific Ocean: The roles of boundary- and wind-driven baroclinic Rossby waves. *Journal of Geophysical Research*, 107 (C12), 1-10.
- <sup>6</sup>Bromirski, P. D., A. J. Miller, R. E. Flick, and G. Auaad, 2011: Dynamical suppression of sea level rise along the Pacific coast of North America: Indications for imminent acceleration. *Journal of Geophysical Research*, 116 (C7), 1-13.
- <sup>7</sup>Strub, P. T. and C. James, 2002: The 1997-1998 oceanic El Niño signal along the southeast and northeast Pacific boundaries: an altimetric view. *Progress In Oceanography*, 54 (1-4), 439-458.
- <sup>8</sup>Lyman, J. M. and G. C. Johnson, 2008: Equatorial Kelvin wave influences may reach the Bering Sea during 2002 to 2005. *Geophysical Research Letters*, 35 (14), 1-5.
- <sup>9</sup>Ramp, S. R., J. L. McClean, C. A. Collins, A. J. Semtner, and K. A. S. Hays, 1997: Observations and modeling of the 1991-1992 El Niño signal off central California. *Journal of Geophysical Research*, 102 (C3), 5553.
- <sup>10</sup>Hermann, A. J., E. N. Curchitser, D. B. Haidvogel, and E. L. Dobbins, 2009: A comparison of remote vs. local influence of El Niño on the coastal circulation of the northeast Pacific. *Deep Sea Research Part II: Topical Studies in Oceanography*, 56 (24), 2427-2443.
- <sup>11</sup>Houston, J. R. and R. G. Dean, 2011: Sea-Level Acceleration Based on U.S. Tide Gauges and Extensions of Previous Global-Gauge Analyses. *Journal of Coastal Research*, 27, 409-417.